THE JOURNAL OF CHEMICAL PHYSICS **140**, 114705 (2014)

Effect of molecular flexibility of Lennard-Jones chains on vapor-liquid interfacial properties

F. J. Blas,[1,2,a)] A. I. Moreno-Ventas Bravo,[2,3] J. Algaba,[1,2] F. J. Martínez-Ruiz,[1,2] and L. G. MacDowell[4]

[1]*Departamento de Física Aplicada, Universidad de Huelva, 21071 Huelva, Spain*
[2]*Centro de Investigación de Física Teórica y Matemática FIMAT, Universidad de Huelva, 21071 Huelva, Spain*
[3]*Departamento de Geología, Facultad de Ciencias Experimentales, Universidad de Huelva, 21071 Huelva, Spain*
[4]*Departamento de Química Física, Facultad de Ciencias Químicas, Universidad Complutense, Madrid 28040, Spain*

(Received 22 December 2013; accepted 26 February 2014; published online 19 March 2014)

We have determined the interfacial properties of short fully flexible chains formed from tangentially bonded Lennard-Jones monomeric units from direct simulation of the vapor-liquid interface. The results obtained are compared with those corresponding to rigid-linear chains formed from the same chain length, previously determined in the literature [F. J. Blas, A. I. M.-V. Bravo, J. M. Míguez, M. M. Piñeiro, and L. G. MacDowell, J. Chem. Phys. **137**, 084706 (2012)]. The full long-range tails of the potential are accounted for by means of an improved version of the inhomogeneous long-range corrections of Janeček [J. Phys. Chem. B **129**, 6264 (2006)] proposed recently by MacDowell and Blas [J. Chem. Phys. **131**, 074705 (2008)] valid for spherical as well as for rigid and flexible molecular systems. Three different model systems comprising of 3, 5, and 6 monomers per molecule are considered. The simulations are performed in the canonical ensemble, and the vapor-liquid interfacial tension is evaluated using the test-area method. In addition to the surface tension, we also obtained density profiles, coexistence densities, critical temperature and density, and interfacial thickness as functions of temperature, paying particular attention to the effect of the chain length and rigidity on these properties. According to our results, the main effect of increasing the chain length (at fixed temperature) is to sharpen the vapor-liquid interface and to increase the width of the biphasic coexistence region. As a result, the interfacial thickness decreases and the surface tension increases as the molecular chains get longer. Comparison between predictions for fully flexible and rigid-linear chains, formed by the same number of monomeric units, indicates that the main effects of increasing the flexibility, i.e., passing from a rigid-linear to a fully flexible chain, are: (a) to decrease the difference between the liquid and vapor densities; (b) to decrease the critical temperature and to increase the critical density; (c) to smooth the density profiles along the interfacial region; (d) to increase the interfacial thickness; and (e) to decrease the vapor-liquid surface tension. © *2014 AIP Publishing LLC*. [http://dx.doi.org/10.1063/1.4868100]

I. INTRODUCTION

Interfacial properties play a key role in many different fields, including nucleation or dynamics of phase transitions, and their knowledge is essential in a great number of practical and industrial applications. This has attracted the attention from simulators of the liquid community over the last years. Among all the interfacial properties, surface tension is obviously the most important and challenging property to be determined and predicted in the context of inhomogeneous systems.[1–3] Despite the great number of studies, especially in the area of computer simulation, the calculation of surface tension remains a subtle problem due to different reasons, being the most important the ambiguity in the definition of the pressure tensor,[1] the finite-size effects due to capillary waves,[4–6] or the difficulty for the calculation of the long-range corrections (LRCs) associated to intermolecular interactions,[7–15] among many others.

The traditional method for determining the fluid-fluid interfacial tension involves the mechanical route through the determination of the normal and tangential pressure tensor profiles using the virial according to different recipes, including those of Irving and Kirkwood[16] and Harasima,[17] among others. See the works of Varnik *et al.*[18] and Ghoufi and Malfreyt[19] for a useful and recent revision of the theoretical background of these methods.

During the last ten years, there has been an intensive and fruitful development of new, elegant, and more effective methodologies for calculating the fluid-fluid interfacial tension. The common point of these methods, different from the standard technique based on the mechanical route, is thermodynamic definition of surface tension. From this point of view, different authors have proposed a new generation of methods and techniques for calculating the surface tension of simple and complex systems, including the Test-Area (TA) method

a)Electronic mail: felipe@uhu.es

of Gloor *et al.*,[20] the Wandering Interface Method (WIM) of MacDowell and Bryk,[21] the Expanded Ensemble technique, originally developed by Lyuvartsev *et al.*[22] and applied by Errington and Kofke[23] and de Miguel,[24] and the Volume Perturbation (VP) methods of de Miguel and Jackson,[25,26] who led to the more general formalism of Brumby *et al.*,[27] recently implemented by Jiménez-Serratos *et al.*,[28] among others.

As new methodologies and techniques were being developed, initially for simple spherical-like models such as systems interacting through the hard-sphere or Lennard-Jones intermolecular potentials, researchers were using and extending these methods for dealing with more complex systems, including chain-like models. In particular, the development of these methods has allowed to study systematically the effect of non-sphericity, and particularly chain length, on different interfacial properties, including vapour-liquid density profiles, interfacial thickness, and surface tension. Special attention has been paid to hydrocarbons, and particular to linear, cyclic, and aromatic alkanes,[29–34] for which very accurate and refined realistic models, under the useful united-atom approximation, were proposed in the middle and late 1990s.[35–43] The existing studies in the literature have provided an in-deep understanding on how the microscopic molecular parameters, mainly the molecular weight or chain length, affect the interfacial behaviour of these systems. However, since the intermolecular potentials are optimized for predicting a given thermodynamic property (normally the vapor-liquid phase behaviour), there has not been any real possibility of studying the effect of flexibility on interfacial properties, specially in simple chain-like models. For instance, the degree of flexibility in alkane models, which is determined by the bending and torsional potentials between chemical groups, is fixed since inter- and intramolecular potentials are optimized to provide the best description of the (vapor-liquid) phase equilibria.

Chain-like molecules are substances formed from monomeric units with a certain degree of flexibility, and n-alkanes molecules and their isomers lie in this general set of molecules. All of them exhibit intramolecular flexibility governed by bending and torsional potentials, that determine the molecular configurations the chains can adopt without overlaps. From a formal point of view, n-alkanes exhibit an intermediate behavior between those shown by two well-known model systems, i.e., the fully flexible (FF)[14,44–48] and rigid-linear (RL) Lennard-Jones (LJ) chain models.[49] The FF chain-like system has neither bending nor torsional potentials between the monomers in a chain. Therefore, there is no energetic penalty when the monomers of the chains adopt a close packed structure at high densities. On the contrary, in the RL chain model the bond length, bond angles, and internal degrees of freedom are fixed. As a consequence of this, both models exhibit completely different phase diagrams, as demonstrated several years ago by Galindo *et al.*[49] A related topic which we do not address here is the influence of bond length flexibility in the phase diagram and interfacial properties, which has been recently studied by Chapela *et al.*[50,51]

During last five years, we have studied the interfacial properties of different simple chain-like molecular models using perturbative methods, such as the WIM and TA methodologies.[14,48,52,53] Very recently,[53] we have determined the interfacial properties of short RLLJ chains from direct simulation of the vapor-liquid interface, including the surface tension using the TA method. In most cases, we have used an improved version[14,53] of the Janeček's method[12] for calculating long-range corrections (LRCs) to the energy in systems that interact through spherically symmetric intermolecular potentials. The main goal of this work is to study the vapor-liquid interfacial properties of short FFLJ chains and compare the results with previous simulation data corresponding to RLLJ obtained by us[53] to determine the effect of molecular flexibility on interfacial properties, with particular emphasis on surface tension. To account for the full intermolecular interactions, we also use the improved method of Janeček[12,14,53] to account for LRCs. To our knowledge, this is the first time the effect of flexibility of Lennard-Jones chains on vapor-liquid interfacial properties is studied from Monte Carlo simulation.

The rest of the paper is organized as follows. In Sec. II we summarize the improved method of Janeček for determining the LRCs of inhomogeneous chain-like systems. The molecular model and the simulation details of this work are presented in Sec. III. Results obtained are discussed in Sec. IV. Finally, in Sec. V we present the main conclusions.

II. EFFECTIVE LONG-RANGE PAIRWISE POTENTIAL FOR MOLECULAR SYSTEMS

In 2006, Janeček[12] proposed a new methodology for calculating long-range corrections (LRC) to the energy in systems that interact through spherically symmetric intermolecular potentials. This procedure allows to treat in a simple way the truncation of the intermolecular energy of systems that exhibit planar interfaces. Three years later, MacDowell and Blas[14] have demonstrated that the Janeček's procedure can be rewritten into an effective long-range pair potential plus a self term that allows for a fast, easy, and elegant implementation of the method. More recently, Blas *et al.*[53] have formally extended the methodology to deal with both FF and RL chain-like molecules. Since the original and improved methodologies have been introduced in Refs. 12–14, we only account here for the most important details of the current version for FFLJ chains.

Consider a system of N chain-like molecules formed from m monomers contained in a volume V that interact through a pairwise intermolecular potential. The total intermolecular potential energy can be written as

$$U = \frac{1}{2}\sum_{i=1}^{N}\sum_{j=1}^{N}\sum_{k=1}^{m}\sum_{k'=1}^{m} u(r_{i,k;j,k'}) = \frac{1}{2}\sum_{i=1}^{N}\sum_{k=1}^{m} U_{i,k}, \qquad (1)$$

where $u(r_{i,k;j,k'})$ is the intermolecular potential between monomer k of molecule i and monomer k' of molecule j, that depends on the distance between the centres of monomers $r_{i,k;j,k'} \equiv |\mathbf{r}_{i,k} - \mathbf{r}_{j,k'}|$. $U_{i,k}$ is the potential energy of a monomer k of the molecule i, which is defined below. During a simulation, the potential energy of a monomer is usually split into two contributions: one arising from the interaction of monomer k in molecule i with all monomers inside a sphere of radius $r_c^{(i,k)}$ centered at this monomer, and a

second term that corresponds to the interaction between the monomer k of molecule i and the rest of monomers forming the system (i.e., all the molecules located outside the cutoff sphere). The potential energy of a monomer k of the molecule i can be then written as

$$U_{i,k} = \sum_{j,k' \in r_c^{(i,k)}} u(r_{i,k;j,k'}) + U_{i,k}^{\mathrm{LRC}}, \tag{2}$$

where the notation $j, k' \in r_c^{(i,k)}$ denotes all the monomers k' of molecules j located inside the cutoff sphere centered at the position of monomer k of molecule i, and $U_{i,k}^{\mathrm{LRC}}$ represents the intermolecular interactions between monomer k of molecule i and the rest of the system due to LRC. Note that $r_c^{(i,k)} \equiv r_c$ since all molecules have the same cutoff distance.

In the improved methodology proposed recently by MacDowell and Blas[14] and Blas *et al.*,[53] the total energy felt by the whole molecule i, due to the long-range interactions with all the molecules that form the system, can be written as

$$U_i^{\mathrm{LRC}} = \sum_{k=1}^{m} U_{i,k}, \tag{3}$$

where $U_{i,k}$ have been previously defined in Eq. (2). U_i^{LRC} can be splitted in different contributions, i.e., intermolecular, intramolecular, and the self-energy contribution,

$$U_i^{\mathrm{LRC}} = U_{i,inter}^{\mathrm{LRC}} + U_{i,intra}^{\mathrm{LRC}} + U_{i,self}^{\mathrm{LRC}}. \tag{4}$$

The intermolecular potential energy between molecule i and the rest of molecules forming the system, due to the LRCs, can be written as

$$U_{i,inter}^{\mathrm{LRC}} = \frac{1}{\mathcal{A}} \sum_{\substack{j=1 \\ (j \neq i)}}^{N} \sum_{k=1}^{m} \sum_{k'=1}^{m} w(|z_{i,k} - z_{j,k'}|). \tag{5}$$

The energy corresponding to the intramolecular interactions associated to segments of molecule i is given by

$$U_{i,intra}^{\mathrm{LRC}} = \frac{1}{\mathcal{A}} \sum_{k=1}^{m-1} \sum_{k'=k+1}^{m} w(|z_{i,k} - z_{i,k'}|). \tag{6}$$

Note that Eq. (6) only takes into account the intramolecular interactions, associated to the LRC, i.e., all possible interactions between segments of molecule i. A long-range contribution from sites in the same molecules is perhaps unexpected, but follows naturally from the fact that long range corrections are implemented here on the basis of segment densities.

And finally, the self-energy contribution to the potential energy of molecule i can be simply written as

$$U_{i,self}^{\mathrm{LRC}} = \frac{1}{\mathcal{A}} \sum_{k=1}^{m} w(0) \equiv \frac{1}{\mathcal{A}} m w(0). \tag{7}$$

The self-energy contribution associated to the long-range interactions given by Eq. (7) is only due to segments belonging to molecule i.

$w(|z_{i,k} - z_{j,k'}|)$ accounts for the intermolecular interactions due to the LRC between a monomer k of molecule i at $z_{i,k}$ and all the monomers k' of all molecules j located inside the slab centered at $z_{j,k'}$. The particular expression for $w(|z_{i,k} - z_{j,k'}|)$ depends on the election of the intermolecular potential of the system. In the original Janeček's method, applicable for molecules interacting through the Lennard-Jones intermolecular potential, the function $w(z)$ is given by

$$w(z) = \begin{cases} 4\pi\epsilon\sigma^2 \left[\frac{1}{5} \left(\frac{\sigma}{r_c} \right)^{10} - \frac{1}{2} \left(\frac{\sigma}{r_c} \right)^{4} \right] & z < r_c \\ 4\pi\epsilon\sigma^2 \left[\frac{1}{5} \left(\frac{\sigma}{z} \right)^{10} - \frac{1}{2} \left(\frac{\sigma}{z} \right)^{4} \right] & z > r_c \end{cases}. \tag{8}$$

The total potential energy of a system of N molecules formed by m segments, due to the long-range interactions, is then calculated as

$$U^{\mathrm{LRC}} = U_{inter}^{\mathrm{LRC}} + U_{intra}^{\mathrm{LRC}} + U_{self}^{\mathrm{LRC}}. \tag{9}$$

The total intermolecular potential energy, due to the long-range interactions, is given by

$$U_{inter}^{\mathrm{LRC}} = \frac{1}{2} \sum_{i=1}^{N} U_{i,inter}^{\mathrm{LRC}} = \frac{1}{2\mathcal{A}} \sum_{i=1}^{N} \sum_{\substack{j=1 \\ (j \neq i)}}^{N} \sum_{k=1}^{m} \sum_{k'=1}^{m} w(|z_{i,k} - z_{j,k'}|)$$

$$= \frac{1}{\mathcal{A}} \sum_{i=1}^{N-1} \sum_{j=i+1}^{N} \sum_{k=1}^{m} \sum_{k'=1}^{m} w(|z_{i,k} - z_{j,k'}|), \tag{10}$$

where we have transformed the unrestricted summation over indexes i and j (with the exception of the case $i = j$ corresponding to intramolecular interactions) into a sum of pairwise effective (integrated) intermolecular potential over all the pair of molecules in the system.

The total intramolecular potential energy due to the long-range interactions is given by

$$U_{intra}^{\mathrm{LRC}} = \sum_{i=1}^{N} U_{i,intra}^{\mathrm{LRC}} = \frac{1}{\mathcal{A}} \sum_{i=1}^{N} \sum_{k=1}^{m-1} \sum_{k'=k+1}^{m} w(|z_{i,k} - z_{i,k'}|). \tag{11}$$

Finally, the total self-energy potential energy due to the long-range interactions is written as

$$U_{self}^{\mathrm{LRC}} = \sum_{i=1}^{N} U_{i,self}^{\mathrm{LRC}} = \frac{1}{\mathcal{A}} \sum_{i=1}^{N} \sum_{k=1}^{m} w(0)$$

$$\equiv \frac{1}{\mathcal{A}} \sum_{i=1}^{N} m w(0) \equiv \frac{1}{\mathcal{A}} N m w(0). \tag{12}$$

Equations (9)–(12) represent the generalization of the improved version of MacDowell and Blas,[14] based on Janeček's method, for the inhomogeneous LRC of chain like systems, including flexible and rigid molecules.[53]

This procedure provides several important advantages over the original method:[53] (1) Eqs. (4)–(7) and (9)–(12) for molecular systems, correspond to the exact evaluation of the intermolecular interactions due to the LRCs, without a discretization of the simulation box along the z-axis; (2) the improved procedure allows to evaluate U_i^{LRC} and U^{LRC} without

the explicit calculation of the density profile on the fly, i.e., it is not necessary to update the density profile $\rho(z)$ each Monte Carlo step; and (3) finally, the implementation of the method is straightforward.

III. MODEL AND SIMULATION DETAILS

We consider chain molecules formed by m identical LJ sites (monomer segments) characterized by a diameter σ and dispersive energy ϵ. The molecules are modeled as FF with monomer-monomer bond length $L = \sigma$, which means that chains are formed by tangent monomers or segments. The interaction potential between two different molecules is given by

$$u^{LJ}(1,2) = \sum_{i=1}^{m}\sum_{j=1}^{m} 4\epsilon\left[\left(\frac{\sigma}{r_{ij}}\right)^{12} - \left(\frac{\sigma}{r_{ij}}\right)^{6}\right], \qquad (13)$$

where r_{ij} is the distance between monomer i of molecule 1 and monomer j of molecule 2. Since we are considering a FF model sites i and j can be in different or in the same molecule, so we are explicitly considering both intermolecular and intramolecular interactions. As previously discussed in the Introduction, we have recently studied a similar model, the RL model. It is important for the discussion of the results in Sec. IV to give here a brief account of the most important features of the model. In this latter system, the molecules are strictly linear and rigid; all intramolecular degrees of freedom are frozen and both the bond distances and bond angles remain fixed. As mentioned previously, in the first model the interactions between segments are identical to those in the RL model, but as the chains are flexible, both intermolecular and in particular intramolecular interactions are now relevant since both contributions are present in the Hamiltonian of the system, as noted before.

We examine a spherically truncated potential model with a cutoff distance of $r_c = 3\sigma$. We consider inhomogeneous LRCs using the MacDowell and Blas[14] recipe (presented in Sec. II), based on the Janeček's method,[12,13] obtaining results for the full LJ potential, i.e., corresponding to infinite truncation distance. According to the discussion of the previous paragraph, since intramolecular interactions are also relevant for this model, we use the full expressions for the inhomogeneous LRC corresponding to U_i^{LRC} and U^{LRC}.

The number of molecules, N, used in each simulation depends on the number of monomers per molecule. We consider $N = 672$, 403, and 336 for systems formed from 3, 5, and 6 monomers, respectively. As in previous studies,[14,48,52,53] this choice is made so as to have systems with the same total number of monomers irrespective of the monomers per molecule. We also compare the results obtained here with those published previously by us[14] corresponding to FF chains formed from 4 monomers (see Sec. IV for further details). Simulations are performed in the NVT ensemble. We consider a system of N molecules at a temperature T in a volume $V = L_x\, L_y\, L_z$, where L_x, L_y, and L_z are the dimensions of the rectangular simulation box. A homogeneous liquid system is first equilibrated in a rectangular simulation box of dimensions $L_x = L_y = 11\sigma$, and $L_z = 24$ for FFLJ chains formed by 3 and 5 monomers, and $L_z = 26$ for chains with 6 monomers. The box is then expanded to three times its original size along the z direction, while leaving the liquid phase at the center. As a result, we obtain a centered liquid slab with those chain bits spanning across the boundary conditions of the original liquid configuration protruding into empty boxes of equal size at each side. The final overall dimensions of the vapor-liquid-vapor simulation box are therefore $L_x = L_y = 11\sigma$, and $L_z = 72$ and 78σ for the corresponding chain lengths.

The simulations are organized in cycles. A cycle is defined as N trial Monte Carlo moves. Our MC procedure comprises three types of configurational updates: one involving a trial displacement of the molecular center of mass, and the other two, a partial and complete molecular regrowth of the molecular chains. For the latter case, we consider a configuration bias scheme.[54,55] Each type of move is chosen with a probability of 20%, 40%, and 40%, respectively. The magnitudes of the appropriate displacements are adjusted so as to get an acceptance rate of 30% approximately. We use periodic boundary conditions in all three directions of the simulation box.

The calculation of the surface tension is performed using of the TA methodology.[20] Since the TA method is a standard and well-known procedure for evaluating the fluid-fluid interfacial tension of liquid, we only provide the most important features of the technique. For further details we recommend the original work[20] and the most important applications.[14,25,26,33,48,56–62] The implementation of the TA technique involves performing test-area deformations of magnitude ΔA during the course of the simulation at constant N, V, and T every MC cycle. As shown by Gloor *et al.*,[20] the surface tension follows from the computation of the change in Helmholtz free energy associated with the perturbation, which in turn can be expressed as an ensemble average of the corresponding Boltzmann factor. Further details can be found in Refs. 14, 20, 48, 52, 53, and 63–66. We consider in all cases two perturbations of size $\Delta A^* = \Delta A/A_0 = \pm 0.0005$, where $A_0 = L_x L_y = 121\sigma^2$ is the interfacial area of the unperturbed state.

As in previous studies,[14,48] for each length we perform simulations of inhomogeneous systems at different temperatures where vapor-liquid equilibrium is expected. We typically consider either eight or nine temperatures in the range $\sim 0.5\, T_c$ up to $\sim 0.9\, T_c$, where T_c is the critical temperature of the system. Each series is started at an intermediate temperature. This system is well equilibrated for 10^6 MC cycles, and averages are determined over a further period of 4×10^6 MC cycles. The systems at other temperatures of each series are equilibrated for 5×10^5 MC cycles and averages are determined over the same number of cycles (4×10^6). The production stage is divided into M blocks. Normally, each block is equal to 10^5 MC cycles. The ensemble average of the surface tension is given by the arithmetic mean of the block averages and the statistical precision of the sample average is estimated from the standard deviation in the ensemble average from $\overline{\sigma}/\sqrt{M}$, where $\overline{\sigma}$ is the variance of the block averages and M has been fixed in this work to $M = 40$.

All the quantities in our paper are expressed in conventional reduced units, with σ and ϵ being the length and energy

scaling units, respectively. Thus, the temperature is given in units of ϵ/k_B, the densities in units of σ^{-3}, the surface tension in units of ϵ/σ^2, and the interfacial thickness in units of σ.

IV. RESULTS AND DISCUSSION

In this section we present the main results from the simulations of FFLJ chains with varying chain length. We focus on the interfacial properties, such as density profiles, interfacial thickness, and surface tension of chains considering a cutoff distance of $r_c = 3\sigma$ and the effective LRCs presented in Sec. II. We also examine the temperature and chain length dependence of these properties. In addition to that, we compare our results obtained for FFLJ chains with those corresponding to RL chain like molecules interacting through the same monomer-monomer intermolecular potential. In particular, we compare the results corresponding to chains formed from 3, 4 (results taken from the work of MacDowell and Blas[14]), and 5 with those obtained recently by Blas *et al.*[53] Results for FF chains with 6 LJ monomers, obtained in the present work, are also presented here for comparison.

We follow the same analysis and methodology than in our previous works,[14,48,53,67] and consider different chain lengths and temperatures. The equilibrium density profiles $\rho(z)$ are computed from averages of the histogram of densities along the z direction over the production stage. Density profiles are given in terms of the monomeric units. The bulk vapor and liquid densities are obtained by averaging $\rho(z)$ over appropriate regions sufficiently removed from the interfacial region. In addition to that, the final bulk vapor density value, at each temperature and chain length, is obtained after averaging the density profiles on both sides of the liquid film. The statistical uncertainty of these values is estimated from the standard deviation of the mean values. Following our previous works, additional interfacial properties, such as the position of the Gibbs-dividing surface, z_0, and the 10-90 interfacial thickness, t, are obtained by fitting each of the two equilibrium density profiles to hyperbolic tangent functions[1] (see Eq. (3) of our previous work[48] for further details). We fix the liquid, ρ_L, and vapor, ρ_V, densities to previously computed values and treat z_0 and t as adjustable parameters. Our simulation results for the bulk densities and interfacial thickness for FFLJ chains formed by 3, 5, and 6 monomers are collected in Table I. The interfacial thickness values summarized here correspond to the average of the values for the two interfaces appearing in the system.

It is important, however, to mention that at high temperature, the density profiles are nearly symmetrical and may be described using a hyperbolic tangent function, as expected in the neighborhood of the critical point.[1] As the temperature is decreased, however, the profiles develop a very strong asymmetry, and the distance from the liquid and vapor densities to the density at the equimolar point is no longer equal.[68] Such asymmetry in the density profile results from the fact that the correlation lengths on the vapor and liquid side are no longer equal far from the critical point, an effect which increases with increasing chain size. As a result, these density profiles may be possible better described using another kind of function, as indicated already by Palanco.[68]

TABLE I. Liquid density ρ_L, vapor density ρ_V, 10-90 interfacial thickness t, and surface tension γ at different temperatures for systems of RLLJ chains formed from m monomers with a monomer-monomer LJ cutoff distance $r_c = 3\sigma$ and inhomogeneous LRCs. All quantities are expressed in the reduced units defined in Sec. III. The errors are estimated as explained in the text.

m	T	ρ_L	ρ_V	t	γ
3	1.20	0.787(2)	0.00093(3)	1.015(2)	0.92(5)
3	1.40	0.724(1)	0.00492(4)	1.3056(9)	0.66(2)
3	1.60	0.6554(3)	0.01674(9)	1.7484(9)	0.429(9)
3	1.80	0.5709(7)	0.0458(1)	2.599(2)	0.224(4)
3	1.85	0.5450(7)	0.0582(2)	2.973(1)	0.171(4)
3	1.90	0.515(1)	0.0744(3)	3.5032(8)	0.131(4)
5	1.00	0.869(3)	0.0000005(3)	0.722(2)	1.28(3)
5	1.20	0.817(2)	0.000024(3)	0.8804(6)	1.04(2)
5	1.40	0.766(1)	0.00031(1)	1.072(1)	0.852(9)
5	1.60	0.7115(8)	0.00193(3)	1.325(2)	0.637(9)
5	1.80	0.6525(6)	0.00737(4)	1.678(2)	0.444(8)
5	2.00	0.5856(6)	0.02138(8)	2.254(3)	0.269(6)
5	2.10	0.5460(7)	0.0346(2)	2.7244(2)	0.205(5)
5	2.20	0.4988(9)	0.0555(4)	3.488(3)	0.140(3)
6	1.00	0.874(5)	0.0000003(9)	0.705(1)	1.40(5)
6	1.20	0.825(3)	0.000004(3)	0.8564(9)	1.12(3)
6	1.40	0.775(2)	0.000087(6)	1.0302(9)	0.89(1)
6	1.60	0.723(1)	0.00072(2)	1.245(2)	0.73(1)
6	1.80	0.6690(7)	0.00337(4)	1.5382(4)	0.501(9)
6	2.00	0.6088(9)	0.01111(6)	1.982(2)	0.351(6)
6	2.20	0.5378(9)	0.0301(1)	2.2772(3)	0.204(6)
6	2.30	0.4938(7)	0.0484(2)	3.523(3)	0.141(4)
6	2.35	0.466(1)	0.0618(5)	4.14(1)	0.114(4)

We show in Fig. 1 the segment density profiles $\rho(z)$ for FFLJ chains formed by three ($m = 3$), five ($m = 5$), and six ($m = 6$) monomers at several temperatures in the vapor-liquid coexistence region. For the sake of clarity, we only present one half of the profiles corresponding to one of the interfaces. Also for convenience, all density profiles have been shifted along z so as to place z_0 at the origin. Since density profiles are expressed in terms of monomeric units in all cases, liquid density increases, and vapor density decreases, at fixed temperature, as the chain length is increased as expected. In addition to that, the absolute value of the slope of the density profiles in the interfacial region decreases as the temperature is increased. This is an expected behavior as temperature approaches to the critical temperature of the system. This is also in agreement with the divergence, as it is shown later, of the interfacial thickness as $T \to T_c$. Another intuitive but less obvious behavior is related with the effect of chain length, at constant temperature, on the slope of the density profile going from the vapor to the liquid phase. As can be seen (it is more obvious at high densities, i.e., $T \sim 1.8$), the slopes of the profiles increase as the chain length is increased from $m = 3$ (Fig. 1(a)) through $m = 4$ (Fig. 1(b)) and $m = 5$ (Fig. 1(c)), and finally up to $m = 6$ (Fig. 1(d)).

Although the behavior of the density profiles of FF chains at different conditions is interesting, it is important to keep in mind that one of the goals of this work is to determine the effect of molecular flexibility on different interfacial properties. A detailed comparison between the density profiles

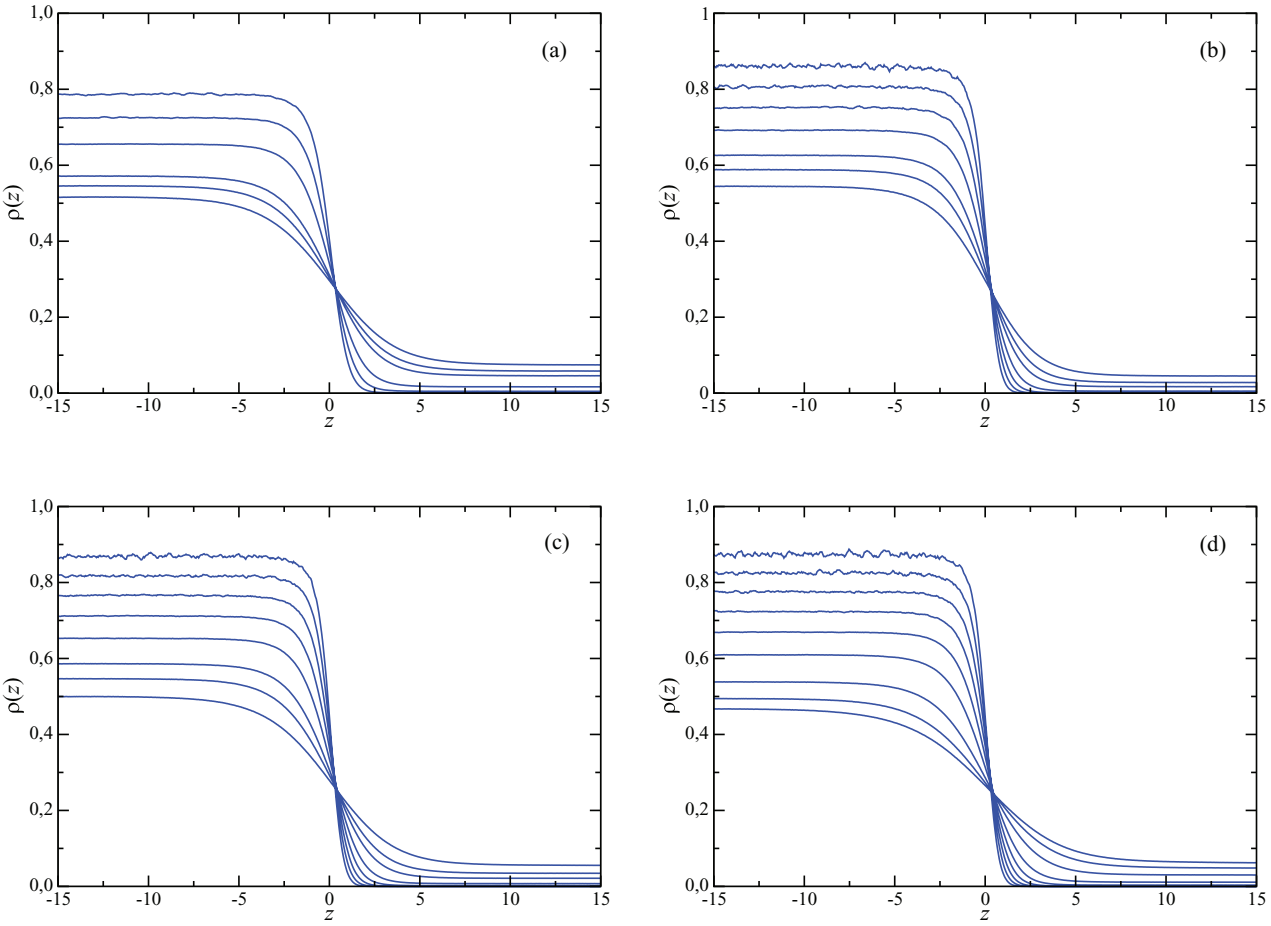

FIG. 1. Simulated equilibrium density profiles across the vapor-liquid interface of FFLJ chains formed from three ($m = 3$) (a), four ($m = 4$) (b), five ($m = 5$) (c), and six ($m = 6$) (d) monomers with a monomer-monomer LJ cutoff of $r_c = 3\sigma$ and inhomogeneous LRCs at several temperatures. From top to bottom (in the liquid region): (a) $T = 1.20$, 1.40, 1.60, 1.80.1.85, and 1.90; (b) $T = 1.00$, 1.20, 1.40, 1.60, 1.80, 1.90, and 2.00; (c) $T = 1.00$, 1.20, 1.40, 1.60, 1.80, 2.00, 2.10, and 2.20; and (d) $T = 1.00$, 1.20, 1.40, 1.60, 1.80, 2.00, 2.20, 2.30, and 2.35.

of FF and RLLJ chains with different chain lengths and temperatures is shown in Figure 2. As can been seen in Figure 2(a), the main effect of flexibility (when comparing density profiles of FF and RLLJ chains formed from four LJ monomers) is to decrease the liquid density, increase the vapor density, and decrease the absolute value of the slope of the density profile along the interfacial region. As can be seen, the change in density is larger in the case of the liquid side than in the vapor side. In addition to that, the changes in density profiles seem to be similar at the two temperatures considered, $T = 1.6$ and 1.9, although the increasing of the vapor density when passing from a RL to a FF change is enhanced as the temperature is increased. This is probably due to the proximity of the critical point of the system ($T_c \sim 2.25$), since the relative changes in vapor and liquid densities as temperature approaches to the critical state are larger in the case of vapor density.

We also consider the effect of flexibility for longer chains ($m = 5$). As can be seen, the same qualitative behavior is observed for the liquid and vapor densities, as well as for the absolute value of the slope of the density profile along the interfacial region. The effect of flexibility is more important and noticeable in this case than in that corresponding to $m = 4$. As can be seen, the change in densities, and especially in the slope (absolute value) of the density profile along the interface is enhanced with respect to that observed for shorter chains ($m = 3$ and 4). Vapor-liquid envelopes of FF and RLLJ chains with $m = 5$ monomers are really different. As demonstrated several years ago by Galindo *et al.*,[49] RLLJ chains exhibit a shrinkage of the liquid range, and that of FFLJ chains present a huge liquid range ($T_t/T_c \sim 0.14$).

We have also estimated the location of the critical point resulting from our direct Monte Carlo simulations. The critical coordinates (temperature, T_c, and density, ρ_c) are obtained following the usual procedure, i.e., using the simulation results for the vapor and liquid coexistence densities (Table I) and the scaling relation for the width of the coexistence curve,[1]

$$\rho_L - \rho_V = A(T - T_c)^{\beta}, \tag{14}$$

and the law of rectilinear diameters

$$\frac{\rho_L + \rho_V}{2} = B + CT. \tag{15}$$

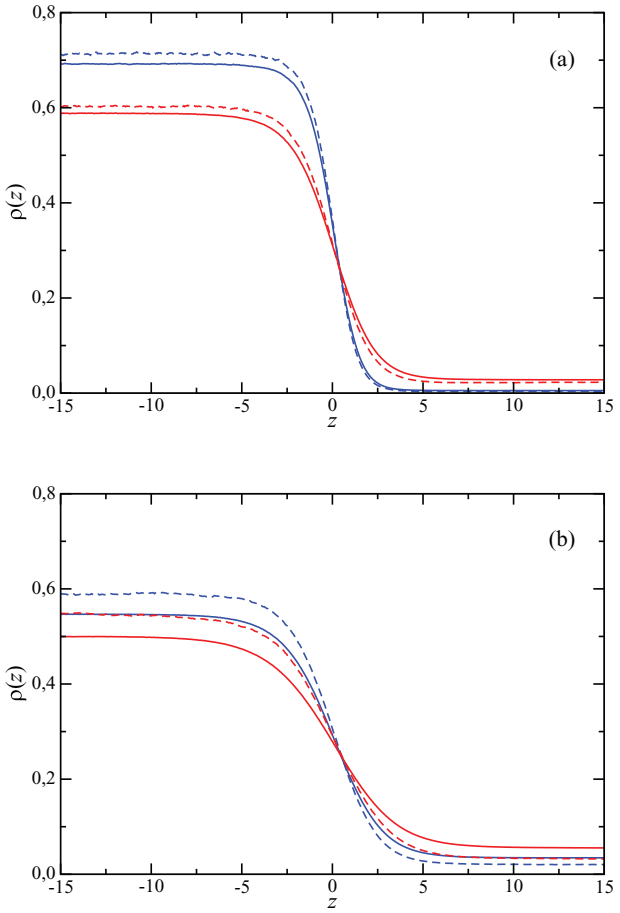

FIG. 2. Simulated equilibrium density profiles across the vapor-liquid interface of FF (continuous curves) and RL (dashed curves) LJ chains formed from: (a) four ($m = 4$) monomers at $T = 1.6$ (blue curves) and $T = 1.9$ (red curves); (b) five ($m = 5$) monomers at $T = 1.9$ (blue curves) and $T = 2.1$ (red curves).

A, B, and C are constants, and β is the corresponding critical exponent. A universal value of $\beta = 0.325$ is assumed here.[1] In Table II we report the values of the critical temperatures and densities as obtained from this procedure for all the systems studied in this work. In addition to that, we have also included the critical conditions (temperature and density) for RLLJ chains formed from 3, 4, and 5 monomers obtained by Blas *et al.*[53]

As a word of caution, we note that the error bars of critical parameters given in Table II are to be considered as the statistical uncertainty resulting from our simulations. In fact, true critical behavior is not seen in finite size simulations, since criticality is governed by a diverging correlation length which in the simulations is limited to the smallest dimension, $L = 11\sigma$. Accordingly, our error bars do not include systematic errors due to finite system size effects.[69] Such errors would need to be studied systematically by means of finite size scaling techniques, as in the works of Wilding and coworkers.[70,71] For the purpose of our work, where we are mainly concerned with the difference between flexible and rigid systems, our results are of sufficient accuracy, however.

TABLE II. Critical densities of FFLJ (ρ_c^{FF}) and RLLJ (ρ_c^{RL}) chains with different chain lengths as obtained from the analysis of the coexistence densities using Eqs. (14) and (15); critical temperatures of FFLJ ($T_c^{FF(a)}$) and RLLJ ($T_c^{RL(a)}$) chains as obtained from the analysis of the coexistence densities using Eqs. (14) and (15); and critical temperatures of FFLJ ($T_c^{FF(b)}$) and RLLJ ($T_c^{RL(b)}$) chains as obtained from the analysis of the computed tension data using Eq. (16) and fixing the critical point to $\mu = 1.258$. All quantities are expressed in the reduced units defined in Sec. III. Results corresponding to RLLJ chains formed by 3, 5, and 6 monomeric units are taken from the work of Blas *et al.*[53] Results corresponding to FFLJ chains formed by four monomeric units ($m = 4$) are taken from the work of MacDowell and Blas.[14]

m	ρ_c^{FF}	ρ_c^{RL}	$T_c^{FF(a)}$	$T_c^{RL(a)}$	$T_c^{FF(b)}$	$T_c^{RL(b)}$
3	0.274(8)	0.27(1)	2.041(9)	2.05(2)	2.09(5)	2.1(2)
4	0.264(7)	0.26(1)	2.26(1)	2.25(3)	2.29(2)	2.3(3)
5	0.253(7)	0.24(2)	2.38(1)	2.50(4)	2.44(2)	2.6(2)
6	0.245(8)	...	2.5(1)	...	2.57(2)	...

The vapor-liquid phase envelopes of FFLJ chains with $r_c = 3\sigma$ and inhomogeneous LRCs are depicted in Fig. 3. We have also included the simulation results corresponding to the coexistence curves of RLLJ chains formed from three ($m = 3$), four ($m = 4$), and five ($m = 5$) monomeric units from our previous work.[53] As previously mentioned, all densities are presented in terms of the monomeric densities since the coexistence curves fall in the same scale when plotted in this way.

We first analyze the phase behavior of FFLJ chains. As can be seen, the phase envelope becomes wider as the chain length is increased from three ($m = 3$) up to six ($m = 6$) segments, as one would expect. Note that we have also included the Monte Carlo simulation results corresponding to the case $m = 4$ (chains formed from four LJ segments) from a previous work.[14] Obviously, the phase envelopes obtained in this work ($m = 3$, 5, and 6) follow the expected intermediate behavior than those corresponding to dimers and chains formed from

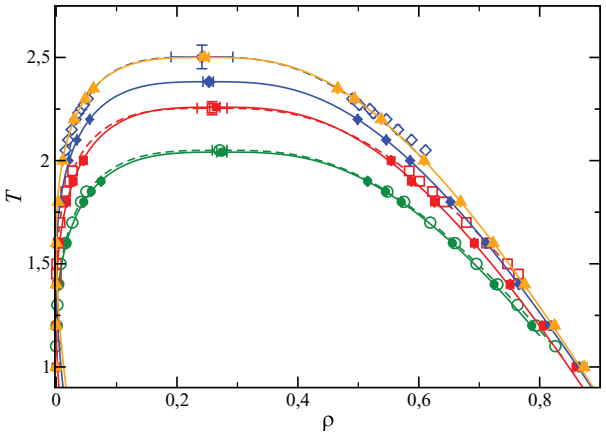

FIG. 3. Vapour-liquid coexistence densities for FF (continuous curves and filled symbols) and RL (dashed curves and open symbols) LJ chains. The open green, red, blue, and orange curves and symbols correspond to the coexistence densities obtained from the MC NVT simulations for chains lengths of $m = 3$, $m = 4$, $m = 5$, and $m = 6$, respectively. The filled red symbols correspond to the existence densities obtained by MacDowell and Blas.[14] Symbols at the highest temperatures for each of the coexistence curve represent the critical points estimated from Eqs. (14) and (15).

eight ($m = 8$) segments. The critical coordinates of chains, for different chain lengths, also follow the expected behavior, i.e., higher critical temperature and lower critical density as the chain length is increased.

Comparison between coexistence curves of FF and RLLJ chains provides interesting conclusions of the effect of molecular flexibility on the phase behavior of chain like systems. As can be seen, the coexistence curves of RLLJ chains exhibit the same qualitative behavior previously explained when the chain length is varied. However, the most interesting conclusions from Fig. 3 arise when comparing the coexistence envelopes of FF and RLLJ chains formed by the same number of monomeric units. As can be seen, the coexistence envelope of RLLJ chains is wider than that corresponding to FF chains, i.e., liquid and vapor densities of RL chains are higher and lower than those of FF, respectively. In addition to that, differences between both phase envelopes increase as the chain length is increased. For instance, for the case of chains formed from three segments ($m = 3$), the phase envelope of both models is nearly equal. However, for chain lengths of $m = 4$, differences are noticeable in both sides of the phase envelope, especially in the liquid side. But the case in which the differences between densities of both models are larger corresponds to $m = 5$, especially at the liquid side of the phase envelope. In summary, the key issue in order to rationalize the different properties between FF and LR chains is that the LR has a higher critical temperature at the same chain length, hence, at a fixed chosen temperature it will be relatively further away from the critical point than the corresponding FF chain. This explains why LR chains have greater segregation, greater surface tension, and smaller interfacial width at a given temperature.

An important difference between the phase envelopes of the two models studied here is the range of temperatures at which vapor-liquid phase equilibria is stable in both models. As the chain length increases, from three ($m = 3$) to five ($m = 5$), the vapor-liquid coexistence range corresponding to the RL chain model is more limited. Contrary, the FFLJ model exhibits a huge liquid range in which vapor and liquid phases coexist, due to the reason previously explained in the Introduction (see also our previous works for further details).[49,53]

This effect can be understood observing the phase behavior of FFLJ chains formed from six ($m = 6$) monomeric units. As can be seen, the range of temperatures at which the system exhibits vapor-liquid separation is huge, from $T \sim 1.0$ up to $T \sim T_c \sim 2.5$. No simulation data for the homologous RL model are available in the literature. We think this model exhibits liquid-crystalline phases for chain lengths equal or larger than six segments, including isotropic, nematic, and smetic phases. Due to this, the determination of the vapor-liquid coexistence properties, and particularly interfacial properties such as surface tension, is a difficult task taking into account that the solid phase would be more stable than the liquid at these conditions.[49,53]

Before presenting the results for other properties it is important to mention the general influence of long-range corrections on the estimation of the critical point. The standard long range corrections to the energy introduce an effective mean field van der Waals like contribution to the Hamiltonian $a\rho^2$. Such behavior is only exact for infinitely long-range pair potentials and produces mean field like criticality.[72] The inhomogeneous long-range corrections introduced here are somewhat more subtle. Indeed, they correspond to an effective infinite long range potential for all pairs of molecules with perpendicular distance $|z_j - z_i| > r_c$, but a finite range potential for pairs of molecules $|z_j - z_i| < r_c$. This most likely also produces mean field critical behavior. However, we use a long range cutoff r_c sufficiently large that the Ising like behavior will dominate the system's behavior except in the close neighborhood of T_c.[73] In practice, this is most likely not an important issue, since we expect that for our limited system sizes finite size effects become relevant before the crossover from Ising like to mean field behavior. As a matter of fact, most estimates for long range r^{-6} potentials that are available in the literature introduce a mean field like character to the simulations by virtue of the homogeneous long range correction to the dispersive energy. In practice, the artifacts that could result are most likely not as important as the suppression of diverging correlation lengths that result from the finite system size.

Another interesting property obtained from our analysis is the 10-90 interfacial thickness, t, of FFLJ chains (cf. Table I). Notice the intrinsic width is not strictly an intrinsic property of the fluid, but rather, increases logarithmically with system size due to the presence of capillary waves.[74] However, our results are performed in all cases for the same lateral size, so that the comparison is meaningful. Furthermore, the lateral system sizes in our simulations are only a few times as large as the fluid's correlation length so that we do not expect for such sizes a large effect of capillary wave broadening. We have also included the results obtained by Blas *et al.*[53] for RLLJ chains formed from three ($m = 3$), four ($m = 4$), and five ($m = 5$) monomeric units. Fig. 4 shows the behavior of the 10-90 interfacial tension, as a function of temperature, for different chain lengths and the

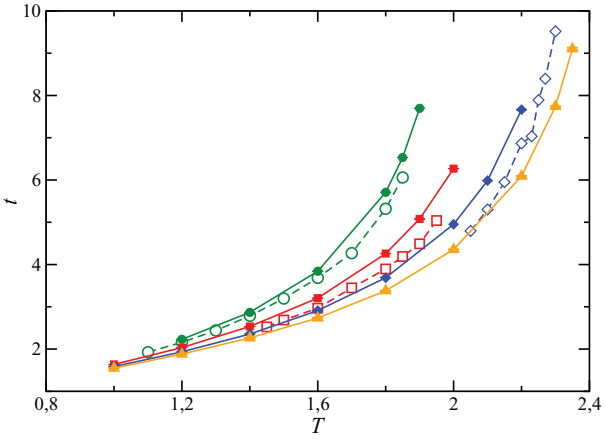

FIG. 4. The 10-90 interfacial thickness t as a function of the temperature for FF (continuous curves and filled symbols) and RL (dashed curves and open symbols) LJ chains. The green, red, blue, and orange colors correspond to the interfacial thickness obtained from the MC NVT simulations for chains lengths of $m = 3$, $m = 4$, $m = 5$, and $m = 6$, respectively. The open symbols correspond to the interfacial thickness obtained by Blas and *et al.*[53] The curves are included as a guide to the eyes.

models considered. As can be seen, for a given chain length, t is seen to increase with temperature, which simply reflects the fact that the interfacial region gets correspondingly wider, as can be also observed in Fig. 2. At low temperatures the density profiles exhibit a sharp interface which corresponds to a low value of the interfacial thickness. As the temperature is increased towards the critical value the interfacial region becomes wider, and hence, the value of the interfacial thickness increases and diverges to infinity as $T \to T_c$. Also note that at low temperatures both surface tension and interfacial widths become very similar for all chain lengths. In this regime of low temperature, the properties of the liquid phase are essentially dictated by packing effects on the scale of segment diameter, which is the same for all chains. It is in this region where Wertheim's thermodynamic perturbation theory and the related SAFT (Statistical Associating Fluid Theory) equation become most accurate,[75–77] as a reference monomer system provides an accurate description of the chain fluid. As the temperature increases, both interfacial width and surface tension are rather dominated by the relative distance from the critical point (cf. Eq. (15)), which is different for each chain, and the properties become very different.

We first concentrate on the behavior of the interfacial tension of FFLJ chains. According to the figure, an increase of the chain length results in a decrease of the thickness of the interface at fixed temperature. The variation of the interfacial thickness, as a function of chain length, is smaller as the chain length increases. In particular, the smallest variation in the interfacial thickness, at a given temperature, occurs when the chain length changes from $m = 5$ to $m = 6$. Note that for intermediate temperatures, $T \sim 1.6$, the interfacial thickness of chains formed from five and six monomeric units is nearly identical. This is a consequence of the scaling behavior observed for FFLJ chains previously shown by different authors.[14,48,52,53,78,79] This behavior is consistent with the shape exhibited by the density profiles associated to the vapor-liquid phase envelopes, which is a consequence of the larger cohesive energy that longer chain like molecules have (in comparison with short chains).

We now consider the difference between the interfacial thickness of FF and RLLJ chains. As can be seen in Fig. 4, the interfacial thickness of flexible chains, at the same temperature and chain length, is larger than that of rigid molecules. The difference between the thickness of flexible and rigid chains, for a fixed chain length, increases as the temperature approaches to the critical temperature of the system. In fact, the difference between both values increases as the chain length is larger. This behavior is consistent with the results shown previously here (see Figs. 1–3).

Finally, it is also important to emphasize one important issue. The range of temperatures at which vapor-liquid phase equilibria is stable in both models is very different. In the case of the flexible model, the system exhibits a huge range in which liquid and vapor coexist. However, the vapor-liquid coexistence range corresponding to the RL chain model is much more limited, as we have explained previously in the Introduction. To recap, the main effect of rigidity on the interfacial thickness of the vapor-liquid coexistence of LJ chains models is to decrease it, especially at temperatures near the critical point and for long-chain systems.

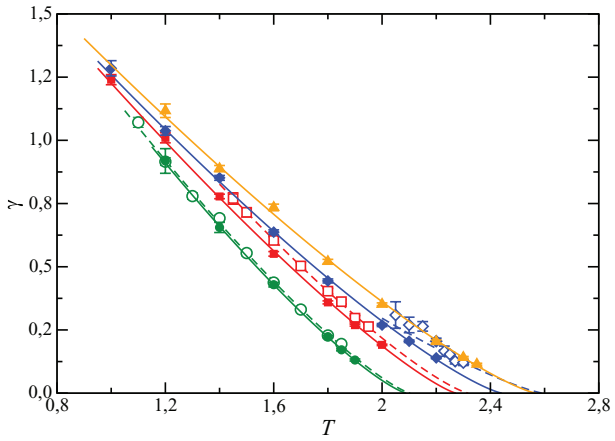

FIG. 5. Surface tension as a function of the temperature for FF (continuous and filled symbols) and RL (dashed curves and open symbols) LJ chains. The green, red, blue and orange colors correspond to the surface tension obtained from the MC NVT simulations for chains lengths of $m = 3$, $m = 4$, $m = 5$, and $m = 6$, respectively. The open symbols correspond to the surface tension obtained by Blas and *et al.*[53] The curves represent the fits of the simulation data to the scaling relationship of the surface tension near the critical point given by Eq. (16) with $\mu = 1.258$.

We finally consider the behavior of the vapor-liquid surface tension of the LJ molecular chains with different sizes. In particular, we compare the results obtained in this work for the FF model with those for RL chains obtained previously.[53] This allows to understand the effect of flexibility of the molecular models on the surface tension of the systems studied. The temperature dependence of the surface tension for flexible and rigid LJ chains is shown in Fig. 5. As can be seen, at any given temperature, the interfacial tension is larger for longer chains. Obviously, this conclusion is valid not only for FF but also for RL chain molecules. Once again, this is consistent with the larger cohesive energy in systems formed by long chains. As can be seen from Fig. 5, an essentially linear behavior is found for the range of temperatures considered here, with a slight curvature close to the critical point for each system. The effect of chain length on the slope of the surface tension curves is remarkable. At a given temperature, this slope becomes less negative as m is increased, a trend which is also exhibited by FFLJ chains,[14,48] as well as by the first members of the n-alkane series.[80] The same qualitative behavior has been previously found by Bryk and collaborators[81] and a previous work.[53]

But probably the most important conclusion of Fig. 5 is the effect of flexibility of similar molecular models, i.e., LJ chains formed from the same number of monomeric units, on the vapor-liquid surface tension. As can be seen clearly, the surface tension increases as the flexibility decreases. In other words, the surface tension of RL molecules is larger than that of FF chains. This is especially noticeable as the chain length increases (particularly for molecules formed from four and five segments). Unfortunately, as we have explained several times along the manuscript, no computer simulation data are available in the literature for RLLJ chains formed by six or more LJ spherical units.

Similar to the case of long FF[14,48] and short RL[53] LJ chains, the computed values of the surface tension allow us to obtain an independent estimate of the critical temperature for each chain length from the scaling relation

$$\gamma = \gamma_0 (1 - T/T_c)^{\mu}, \tag{16}$$

where γ is the surface tension at temperature T, γ_0 is the "zero-temperature" surface tension, μ is the corresponding critical exponent, and T_c is the critical temperature. Here, we fix μ to the universal value of $\mu = 1.258$ as obtained from renormalization-group theory.[1] Our estimates for the critical temperatures are collected in Table II. The overall agreement between these values and those obtained from an analysis of the coexistence densities is satisfactory. It is also possible to compare these results with predictions obtained previously by Blas *et al.*[53] corresponding to the RLLJ molecular chain model. As can be seen in Table II, the same conclusion obtained previously from the analysis of the coexistence densities is also observed here: the main effect of flexibility on the critical point is to decrease the critical temperature of the chain model, with the same number of monomeric units, with respect to that of the rigid one.

It is interesting to mention here that, although the surface tension values of FF and RL chains are different, at the same temperature and for molecules formed from the same number of monomeric units, we have recently found[52] that it is possible to find a universal scaling relationship to correlate short- and long-chains molecules with different degrees of flexibility and interacting through different intermolecular potentials (Lennard-Jones and square-well potentials).

Before presenting the conclusions of this work, it is interesting to comment some issues about the scaling properties we have investigated. In particular, we have considered scaling relationships for the vapor-liquid and interfacial tension but not for the interfacial width. As it is well-known, in the van der Waals theory of interfaces, the interfacial width is readily identified with the bulk correlation length. Accordingly, we could try to test the expected scaling law for the correlation length $\xi \propto t^{-\nu}$, where $t = 1 - T/T_c$, using our data for the interfacial width. However, the van der Waals theory, as other mean field theories, miss the role of capillary waves. Such waves result in an interfacial broadening which is larger than the bulk correlation length and depends on the system size. Indeed, it is expected that the interfacial width obeys $\xi^2 = \xi_0^2 + \xi_{\rm cw}^2$, where ξ_0 is the bulk correlation length, which scales as $t^{-\nu}$, while an additional interfacial broadening stemming from capillary waves is $\xi_{\rm cw}^2 = k_B T/2\pi\gamma_{\rm lv} \ln L q_{\rm max}$, where $q_{\rm max}$ is an upper wave-vector cutoff. Accordingly, the scaling form of the interfacial width is governed by both ν and $\mu \approx 2\nu$. Far away from the critical point, clearly terms of order $t^{-\nu}$ will be important, but close to the critical point a divergence of order $t^{-\mu}$ should occur. Unfortunately, the analysis of the data obtained from simulations does not give conclusive results.

V. CONCLUSION

We have determined the interfacial properties of the vapor-liquid interface of short FFLJ chains formed from tangentially bonded monomers. Chains formed by three, five, and six monomers are considered. The intermolecular monomer-monomer interactions are truncated at a cutoff distance of three times the segment size of the monomers forming the chains. We use an improved version of the Janeček methodology proposed recently by MacDowell and Blas that allows to evaluate the long-range corrections to the potential energy as an effective pairwise intermolecular potential, without need of the explicit calculation of the current density profile along the simulation. We use Monte Carlo *NVT* simulations of the inhomogeneous system containing two vapor-liquid interfaces. The surface tension is evaluated using the TA approach. We have examined the density profiles, interfacial thickness, and surface tension in terms of the temperature and the number of monomers forming the chains. In addition, we have also calculated the coexistence phase envelope, including the location of the critical point from an analysis of the density profiles and the surface tension. In addition to that, we have compared the results obtained with those corresponding to RLLJ chains formed from the same number of monomeric segments previously determined in the literature.

The effect of the chain length on the density profiles, coexistence densities, critical temperature and density, interfacial thickness, and surface tension has been investigated. The vapor-liquid interface is seen to sharpen with increasing chain length corresponding to an increase in the width of the coexistence phase envelope, and an accompanying increase in the surface tension. The vapor-liquid surface tension of RLLJ chains is seen to exhibit a universal scaling behavior when is appropriately reduced with respect to the chain length and critical density and temperature, and represented as a function of the difference between the vapor and liquid coexistence densities (relative to the critical point).[52]

Comparison between predictions for FFLJ and RLLJ with the same number of monomeric segments indicates that the flexibility of the chains affects both vapor-liquid coexistence and interfacial properties. In particular, from the thermodynamic point of view, the difference between the liquid and vapor coexistence densities decreases when passing from a RL to FF chain, with a decrease of the critical temperature and a decrease of the critical density. From the point of view of the interfacial properties, the density profiles become smoother along the interfacial region as the flexibility is increased, with the corresponding enlargement of the region in which the liquid changes continuously to vapor. This increasing of interfacial thickness produces a small decrease of the vapor-liquid surface tension for short chains, which becomes larger as the chain length is increased.

ACKNOWLEDGMENTS

The authors would like to acknowledge helpful discussions with C. Vega, A. Galindo, J. M. Míguez, and M. M. Piñeiro. This work was supported by Ministerio de Ciencia e Innovación (MICINN, Spain) through Grant Nos. FIS2011-13119-E, FIS2010-14866 (F.J.B. and F.J.M.R.), and FIS2010-22047-C05-05 (L.G.M.D.). Further financial support from Proyecto de Excelencia from Junta de Andalucía (Grant No. P07-FQM02884), Comunidad Autónoma de Madrid

(Grant No. MODELICO-P2009/EPS-1691), and Universidad de Huelva is also acknowledged.

[1]J. S. Rowlinson and B. Widom, *Molecular Theory of Capillarity* (Claredon Press, 1982).
[2]D. Henderson, *Fundamentals of Inhomogeneous Fluids* (Dekker, New York, 1992).
[3]H. T. Davis, *Statistical Mechanics of Phases, Interfaces, and Thin Films* (VCH, Weinheim, 1996).
[4]K. Binder, Z. Phys. B Condens. Matter **43**, 119 (1981).
[5]A. Aguado, W. Scott, and P. A. Madden, J. Chem. Phys. **115**, 8612 (2001).
[6]L.-J. Chen, J. Chem. Phys. **103**, 10214 (1995).
[7]E. M. Blokhuis, D. Bedeaux, C. D. Holcomb, and J. A. Zollweg, Mol. Phys. **85**, 665 (1995).
[8]M. Mecke, J. Winkelmann, and J. Fischer, J. Chem. Phys. **107**, 9264 (1997).
[9]M. Mecke, J. Winkelmann, and J. Fischer, J. Chem. Phys. **110**, 1188 (1999).
[10]K. C. Daoulas, V. A. Harmandaris, and V. G. Mavrantzas, Macromolecules **38**, 5780 (2005).
[11]M. Guo and B. C.-Y. Lu, J. Chem. Phys. **106**, 3688 (1997).
[12]J. Janeček, J. Phys. Chem. B **110**, 6264 (2006).
[13]J. Janeček, H. Krienke, and G. Schmeer, J. Phys. Chem. B **110**, 6916 (2006).
[14]L. G. MacDowell and F. J. Blas, J. Chem. Phys. **131**, 074705 (2009).
[15]R. de Gregorio, J. Benet, N. A. Katcho, F. J. Blas, and L. G. MacDowell, J. Chem. Phys. **136**, 104703 (2012).
[16]J. H. Irving and J. G. Kirkwood, J. Chem. Phys. **18**, 817 (1950).
[17]A. Harasima, Adv. Chem. Phys. **1**, 203 (1958).
[18]F. Varnik, J. Baschnagel, and K. Binder, J. Chem. Phys. **113**, 4444 (2000).
[19]A. Ghoufi and P. Malfreyt, Mol. Simul. **39**, 603 (2013).
[20]G. J. Gloor, G. Jackson, F. J. Blas, and E. de Miguel, J. Chem. Phys. **123**, 134703 (2005).
[21]L. G. MacDowell and P. Bryk, Phys. Rev. E **75**, 061609 (2007).
[22]A. P. Lyuvartsev, A. A. Martsinovski, S. V. Shevkunov, and P. N. Vorontsov-Velyaminov, J. Chem. Phys. **96**, 1776 (1992).
[23]J. R. Errington and D. A. Kofke, J. Chem. Phys. **127**, 174709 (2007).
[24]E. de Miguel, J. Phys. Chem. B **112**, 4674 (2008).
[25]E. de Miguel, F. J. Blas, and E. M. del Río, Mol. Phys. **104**, 2919 (2006).
[26]E. de Miguel and G. Jackson, J. Chem. Phys. **125**, 164109 (2006).
[27]P. E. Brumby, A. J. Haslam, E. de Miguel, and G. Jackson, Mol. Phys. **109**, 169 (2011).
[28]G. Jiménez-Serratos, C. Vega, and A. Gil-Villegas, J. Chem. Phys. **137**, 204104 (2012).
[29]F. Goujon, P. Malfreyt, A. Boutin, and A. H. Fuchs, Mol. Simul. **27**, 99 (2001).
[30]F. Goujon, P. Malfreyt, A. Boutin, and A. H. Fuchs, J. Chem. Phys. **116**, 8106 (2002).
[31]F. Goujon, P. Malfreyt, J.-M. S. A. Boutin, B. Rousseau, and A. H. Fuchs, J. Chem. Phys. **121**, 12559 (2004).
[32]C. Ibergay, A. Ghoufi, F. Goujon, P. Ungerer, A. Boutin, B. Rousseau, and P. Malfreyt, Phys. Rev. E **75**, 051602 (2007).
[33]F. Biscay, A. Ghoufi, F. Goujon, and P. Malfreyt, J. Phys. Chem. B **112**, 13885 (2008).
[34]F. Biscay, A. Ghoufi, V. Lachet, and P. Malfreyt, Phys. Chem. Chem. Phys. **11**, 6132 (2009).
[35]B. Smit, S. Karaborni, and J. I. Siepmann, J. Chem. Phys. **102**, 2126 (1995).
[36]J. I. Siepmann, S. Karaborni and B. Smit, J. Am. Chem. Soc. **115**, 6454 (1993).
[37]J. I. Siepmann, S. Karaborni and B. Smit, Nature (London) **365**, 330 (1993).
[38]J. I. Siepmann, M. G. Martin, C. Mundy, and M. L. Klein, Mol. Phys. **90**, 687 (1997).
[39]M. G. Martin and J. I. Siepmann, J. Am. Chem. Soc. **119**, 8921 (1997).
[40]M. G. Martin and J. I. Siepmann, J. Phys. Chem. B **102**, 2569 (1998).
[41]C. Vega and A. L. Rodríguez, J. Chem. Phys. **105**, 4223 (1996).
[42]A. López-Rodríguez, C. Vega, and J. J. Freire, J. Chem. Phys. **111**, 438 (1999).
[43]S. K. Nath, F. A. Escobedo, and J. J. de Pablo, J. Chem. Phys. **108**, 9905 (1998).
[44]Y.-J. Sheng, A. Z. Panagiotopoulos, S. K. Kumar, and I. Szleifer, Macromolecules **27**, 400 (1994).
[45]Y.-J. Sheng, A. Z. Panagiotopoulos, and S. K. Kumar, Macromolecules **29**, 4444 (1996).
[46]F. Escobedo and J. J. de Pablo, Mol. Phys. **87**, 347 (1996).
[47]D. Duque, J. C. Pàmies, and L. F. Vega, J. Chem. Phys. **121**, 11395 (2004).
[48]F. J. Blas, L. G. MacDowell, E. de Miguel, and G. Jackson, J. Chem. Phys. **129**, 144703 (2008).
[49]A. Galindo, C. Vega, E. Sanz, L. G. MacDowell, E. de Miguel, and F. J. Blas, J. Chem. Phys. **120**, 3957 (2004).
[50]G. A. Chapela and J. Alejandre, J. Chem. Phys. **135**, 084126 (2011).
[51]G. A. Chapela, E. Díaz-Herrera, J. C. Armas-Pérez, and J. Quintana-H, J. Chem. Phys. **138**, 224509 (2013).
[52]F. J. Blas, F. J. Martínez-Ruiz, A. I. M.-V. Bravo, and L. G. MacDowell, J. Chem. Phys. **137**, 024702 (2012).
[53]F. J. Blas, A. I. M.-V. Bravo, J. M. Míguez, M. M. Piñeiro, and L. G. MacDowell, J. Chem. Phys. **137**, 084706 (2012).
[54]D. Frenkel and B. Smit, *Understanding Molecular Simulations*, 2nd ed. (Academic, San Diego, 2002).
[55]J. J. de Pablo, M. Laso, and U. W. Suter, J. Chem. Phys. **96**, 2395 (1992).
[56]C. Vega and E. de Miguel, J. Chem. Phys. **126**, 154707 (2007).
[57]J. M. Míguez, D. González-Salgado, J. L. Legido, and M. M. Piñeiro, J. Chem. Phys. **132**, 184102 (2010).
[58]G. Galliero, M. M. Piñeiro, B. Mendiboure, C. Miqueu, T. Lafitte, and D. Bessières, J. Chem. Phys. **130**, 104704 (2009).
[59]E. de Miguel, N. G. Almarza, and G. Jackson, J. Chem. Phys. **127**, 034707 (2007).
[60]C. Miqueu, J. M. Míguez, M. M. Piñeiro, T. Lafitte, and B. Mendiboure, J. Phys. Chem. B **115**, 9618 (2011).
[61]F. Biscay, A. Ghoufi, F. Goujon, V. Lachet, and P. Malfreyt, J. Chem. Phys. **130**, 184710 (2009).
[62]F. Biscay, A. Ghoufi, V. Lachet, and P. Malfreyt, J. Chem. Phys. **131**, 124707 (2009).
[63]J. G. Sampayo, A. Malijevský, E. A. Müller, E. de Miguel, and G. Jackson, J. Chem. Phys. **132**, 141101 (2010).
[64]J. M. Míguez, M. M. Piñeiro, A. I. M.-V. Bravo, and F. J. Blas, J. Chem. Phys. **136**, 114707 (2012).
[65]J. M. Míguez, M. M. Piñeiro, and F. J. Blas, J. Chem. Phys. **138**, 034707 (2013).
[66]F. J. Blas and B. Mendiboure, J. Chem. Phys. **138**, 134701 (2013).
[67]J. G. Sampayo, F. J. Blas, E. de Miguel, E. A. Müller, and G. Jackson, J. Chem. Eng. Data **55**, 4306 (2010).
[68]J. M. G. Palanco, "Termodinámica estadística de fluidos moleculares y sus interfases," Ph.D. thesis (Universidad Complutense de Madrid, 2013).
[69]K. Binder, Rev. Prog. Phys. **50**, 783 (1987).
[70]N. B. Wilding, Phys. Rev. E **52**, 602 (1995).
[71]N. B. Wilding, M. Müller, and K. Binder, J. Chem. Phys. **105**, 802 (1996).
[72]G. J. Pauschenwein, J. M. Caillol, D. Levesque, J. J. Weis, E. Scholl-Paschinger, and G. Kahl, J. Chem. Phys. **126**, 014501 (2007).
[73]E. Luijten and K. Binder, Phys. Rev. E **58**, R4060 (1998).
[74]L. G. MacDowell, J. Benet, N. A. Katcho, and J. M. G. Palanco, Adv. Colloid Interface Sci. **206**, 150 (2014).
[75]F. J. Blas and L. F. Vega, Mol. Phys. **92**, 135 (1997).
[76]F. J. Blas and L. F. Vega, J. Chem. Phys. **115**, 4355 (2001).
[77]L. G. MacDowell, P. Virnau, M. Müller, and K. Binder, J. Chem. Phys. **117**, 6360 (2002).
[78]C. Vega and L. G. MacDowell, J. Chem. Phys. **114**, 10411 (2001).
[79]C. Vega, F. J. Blas, and A. Galindo, J. Chem. Phys. **116**, 7645 (2002).
[80]G. J. Gloor, G. Jackson, F. J. Blas, E. M. del Río, and E. de Miguel, J. Phys. Chem. C **111**, 15513 (2007).
[81]P. Bryk, K. Bucior, S. Sokolowski, and G. Zukocinski, J. Phys. Condens. Matter **16**, 8861 (2004).